Publ. Astron. Soc. Aust., 1998, 15, 318–24

Observational Tests of a Double Loop Model for Solar Flares

S. J. Hardy[1], D. B. Melrose[1] and H. S. Hudson[2,3]

[1]Research Centre for Theoretical Astrophysics,
School of Physics, University of Sydney, NSW 2006, Australia
S.Hardy, D.Melrose@physics.usyd.edu.au
[2]Solar Physics Research Corp., 4720 Calle Desecada, Tucson, AZ 85718, USA
[3]ISAS, 3–1-1 Yoshinodai, Sagamihara, Kanagawa 229, Japan
hudson@iasass0.solar.isas.ac.jp

Received 1997 December 29, accepted 1998 August 17

Abstract: A model for the energetics of solar flares, developed by Melrose (1997), is based on magnetic reconnection between two current-carrying magnetic loops. A detailed numerical investigation of the model has been made to identify those configurations that lead to energy release in a flare. Our results predict a strong relation between the ratio of currents in the interacting loops for a favoured flare configuration, and provide further support for a proposed method of generating long loops connecting different active regions. Both of these predictions are amenable to observational verification.

Keywords: Sun: flares — magnetic reconnection — magnetic flux loops

1 Introduction

The suggestion that many solar flares are due to the interaction of two or more flux loops interacting within an active region is longstanding (e.g. Heyvaerts, Priest & Rust 1977; Machado et al. 1988). Recently, Nishio et al. (1997) and Hanaoka (1997) used a combination of microwave, soft X-ray and magnetogram observations to demonstrate that a large number of solar flares occur where a new flux loop emerges within an active region and interacts with an existing loop, presumably through magnetic reconnection. The structure suggested by these observations is that of the interaction of at least two current- and flux-carrying loops, each with a footpoint where current emerges from the photosphere and a footpoint where current re-enters the photosphere. The relative motion of these loops causes them to intersect and exchange currents and flux through the process of magnetic reconnection. This picture has been expanded into a model by Melrose (1997; hereinafter M97), who explored in detail the implications of the fact that within this model the strengths of currents moving through the footpoints of the loops cannot change significantly over the timescale of a flare. This constraint implies that the energy release in the flares is due solely to a redistribution of current and flux above the photosphere.

The model of M97 relates the geometry of the footpoints of the loops and the currents within the loops to the total energy released by the flare. A proviso is that the dominant contribution to the energy released by the flare must be due to the change in magnetic energy associated with the redistribution of currents between the footpoints of the loops. There is also a change in the magnetic energy associated with transfer of flux between the loops, but it was argued by M97 that this is a smaller effect, and it is ignored here. Using the model of M97, any particular configuration of footpoints can be modelled and an estimate of the energy released can be made. If the energy difference, $\Delta E = E_{\rm pre} - E_{\rm post}$, between the pre- and post-current-transfer states is positive, it is assumed that a flare may occur, with this energy available through magnetic reconnection. If the energy difference is negative, no flare should occur. There is a further condition for a flare to occur: the loop structures must intersect, in order for the reconnection and the current transfer to be possible.

The efficacy of the model of M97 can only be determined through comparison with the observational data on flares. The purpose of this paper is to explore the observable consequences of this model, and to propose strategies whereby existing and future instrumentation may explore the correctness of its predictions. The structure of this paper is as follows. In Section 2, the model for solar flares presented in M97 is outlined briefly. This is followed in Section 3 with the application of the model to a variety of footpoint configurations.

 1323-3580/98/030318$05.00

Section 4 contains the conclusions that are drawn from this work.

2 Current Redistribution Model for Flares

The model proposed in M97 is that solar flares occur when two current-carrying flux loops interact. Current and flux are transferred between the loops by magnetic reconnection. The energy released is determined by the difference between the magnetic energy stored in the current configuration before and after the flare. It is important to note that the timescale of flares is such that the currents through the photosphere do not have time to change over the course of the flare. This implies that only the photospheric boundary conditions on the magnetic field and the current are fixed by the initial conditions, and that subphotospheric processes play no role during the flare.

2.1 The Model

Consider the current geometry shown in Figure 1. Four footpoints are shown on the solar photosphere where current and magnetic flux either emerge or re-enter. Before the flare, there are two current-carrying loops between these footpoints, with some point of intersection at which reconnection occurs. During the flare some of the current, ΔI, and some of the flux, $\Delta\Psi$, is transferred from the initial loops to new loops connecting the footpoints. The energy released through the current transfer shown in Figure 1 is given by

$$\Delta E = R\Delta I + M^{\rm IR}(\Delta I)^2 \,, \qquad (1)$$

where

$$R = M_1^{\rm LCS}(I_1 - \Delta I) + M_2^{\rm LCS}(I_2 - \Delta I) \,, \qquad (2)$$

with

$$M_n^{\rm LCS} = M_{n1} + M_{n2} + M_{n3} + M_{n4} \,, \qquad (3)$$

$$M^{\rm IR} = \tfrac{1}{2}(L_1 + L_2 - L_3 - L_4) + M_{12} - M_{34} \,, \qquad (4)$$

and where M_{ij} denotes the mutual inductances of the current carrying loops, and $L_i = M_{ii}$ are the self-inductances of the current-carrying loops. The indexing of the loops is given by $1 : (1+ \rightarrow 1-)$, $2 : (2+ \rightarrow 2-)$, $3 : (1+ \rightarrow 2-)$, and $4 : (2+ \rightarrow 1-)$ where the footpoints are labelled as in Figure 1. The division of equation (1) into *irreducible reconnection* (IR) and *like-current separation* (LCS) terms is discussed further in M97.

Equation (1) is the basis of the model of M97. If ΔE is positive, the geometry of the situation is such that a current transfer leads to a net release of energy, and a flare is expected. However, if ΔE is negative, a redistribution of currents would lead to a net increase of energy and would need another source of energy to drive it. Such a change could not occur spontaneously, and such configurations should not produce a flare.

There is a maximum allowed current transfer, imposed by the requirement that the photospheric currents do not change, equal to the minimum of the currents flowing in the initial loops. (Note that M97 is in error when it says that the maximum current transferred is $|I_1 - I_2|$.) As particular loop structures within active regions may undergo multiple flaring events, the maximum current need not be transferred in a single flare. However, for the configurations investigated here, ΔE scales monotonically with the magnitude of the current transfer. Thus, assuming that maximal current transfer does take place allows the geometries that produce flares to be identified, without introducing a parameter representing the fraction of the maximal current that is transferred. Maximal current transfer is assumed throughout unless otherwise stated.

2.2 Mutual Inductances of the Loops

The mutual inductances of the current-carrying chromospheric loops are defined by the current distributions within the loops. Clearly some approximation must be made to these to treat flares in any generality. M97 assumed that the loops are approximated as half-tori which are aligned

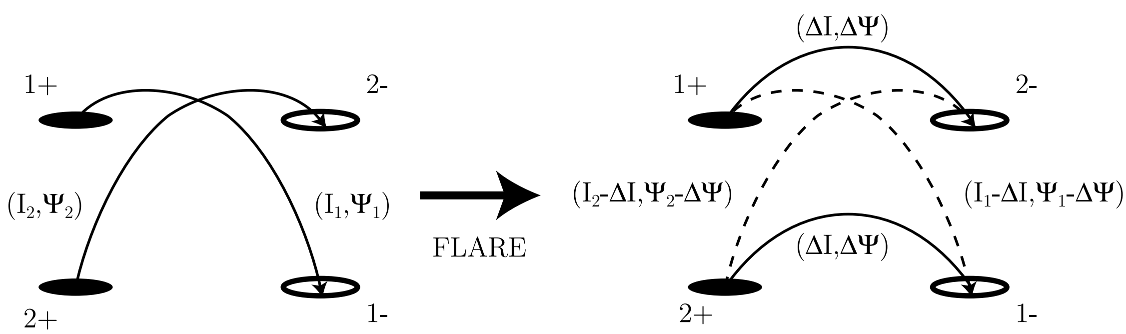

Figure 1—Sketch of model of current and flux redistribution during a solar flare. The energy released during the flare is identified with the change of magnetic energy associated with the redistribution of currents above the photosphere.

https://doi.org/10.1071/AS98318

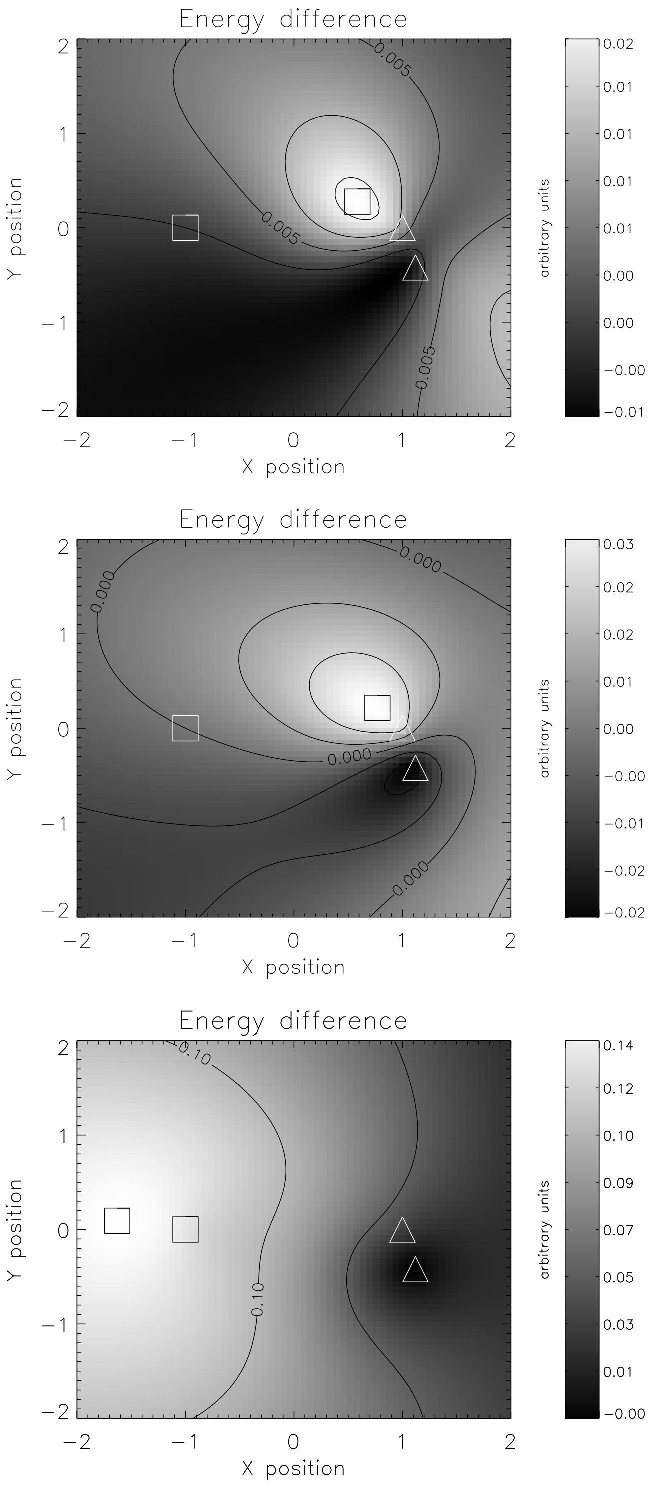

Figure 2—Plots of the fractional energy release due to maximal current redistribution between two loops. The axes represent two-dimensional spatial coordinates on the solar surface, with arbitrary units. Positive-polarity footpoints are represented by squares, and negative-polarity footpoints are represented by triangles. In all three plots one initial current loop between $(-1, 0)$ and $(1, 0)$ is fixed with current I_1, and the second initial current loop has a single fixed negative-polarity footpoint at $(1{\cdot}12, -0{\cdot}42)$, a positive-polarity footpoint which varies over the plot, and a current I_2 carried between them. The current ratios $r = I_1/I_2$ in the three plots are 3, 1 and 1/3 respectively. The actual values in the plot are scaled by $\mu_0 C(I_1 + I_2)^2$. Note that for all three current ratios, energy is released for parasitic topologies such as that seen in Figure 4. The second square marks the position of the 2+ footpoint corresponding to maximum energy release.

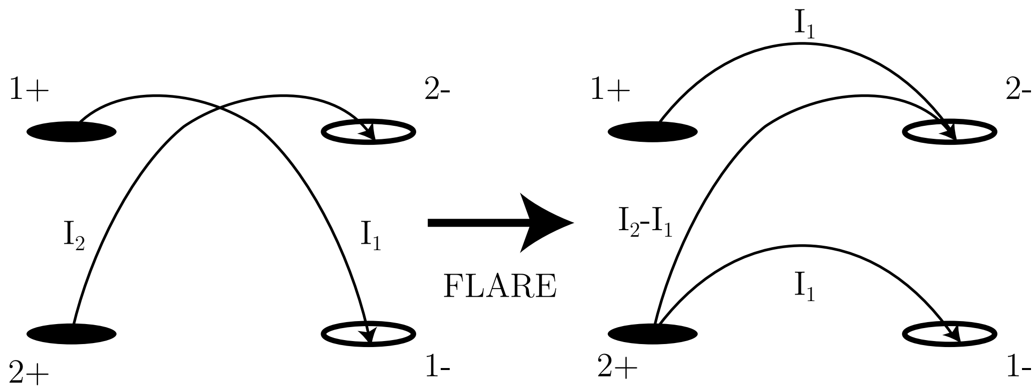

Figure 3—Sketch of the model of maximal current transfer between the loops, assuming $I_1 < I_2$.

vertically with respect to the photosphere. The self-inductance of a loop with major radius a_n and minor radius r_n is given by (Landau & Lifshitz 1960, p. 139)

$$L_n = \mu_0 C a_n \,, \tag{5}$$

with

$$C = \tfrac{1}{2}\left(\ln \frac{8a_n}{r_n} - \tfrac{7}{4}\right) . \tag{6}$$

The term $\frac{7}{4}$ corresponds to a uniform current profile.

The mutual inductance between two loops has not been solved analytically for a general configuration of the loops. There are, however, a number of limiting cases, and M97 presented an interpolation formula between these known results. Consider two loops of major radii a_m and a_n, with centres separated by d_{mn}, and which are oriented with an angle θ_{mn} between them. The interpolation formula derived in M97 is

$$M_{mn} = \mu_0 C \frac{8a_n^2 a_m^2 \cos\theta_{mn}}{[(a_m + a_n)^2 + d_{mn}^2]^{\frac{3}{2}}} . \tag{7}$$

The interpolation formula, equation (7), is used here in the calculation of the energy difference between the pre- and post-flare states.

3 Application of Model

We report a detailed investigation of the loop configurations in which the occurrence of solar flares is preferred. The general approach is graphical, in that the phase space to be explored is four dimensional: the location of two footpoints may be fixed, leaving two footpoints to be varied, and there is a further parameter which is the ratio of the currents in the two loops. There is a degeneracy in these parameters as the scaling of the system is arbitrary, reducing the five free parameters to four.

One idea is to search for the maxima of the energy release according to equation (1). However, this proves unfruitful as the most favourable conditions are often those where one of the loops is longest. Thus there is no global maximum, as ΔE increases as one of the footpoints is moved toward infinity, and the other footpoints remain fixed.

A more productive method of looking for geometries that are favourable for energy release through flares involves fixing three of the footpoints and the ratio of currents between the loops, and then plotting ΔE as a function of the location of the fourth footpoint. Here we assume that maximal current transfer occurs. This leads to plots of the type shown in Figure 2, where footpoints 1+ and 1− are at $(-1, 0)$ and $(1, 0)$ respectively, footpoint 2− has been fixed at $(1{\cdot}12, -0{\cdot}42)$, and footpoint 2+ is allowed to vary. Those regions that are light correspond to positions for which there is a net release of magnetic energy if a flare occurs. The squares denote the footpoints of positive polarity, and the triangles denote the footpoints of negative polarity.

The dark regions of Figure 2 correspond to those configurations that have higher magnetic energy in their final state. For maximal current transfer, this final state is shown in Figure 3. Thus, the dark regions of Figure 2 correspond to configurations where reconnection of three loops to form two loops is favourable.

3.1 Parasitic Topology

A C9·1 flare event displaying 'parasitic magnetic topology' is shown in Figure 4. This flare was analysed in detail by Hanaoka (1997). The observations show an emerging flux loop at the right-hand footpoint of the long loop. This emerging loop interacts with the existing loop, appearing to cause a flare. Many flares exhibit this behaviour, and several of these were analysed recently by Nishio et al. (1997) and Hanaoka (1997). We explore this class of events using the model of M97. In particular, we take the geometry suggested in Figure 4 as the base configuration for our exploration, and extrapolate from these results an observational test of the model of M97.

https://doi.org/10.1071/AS98318

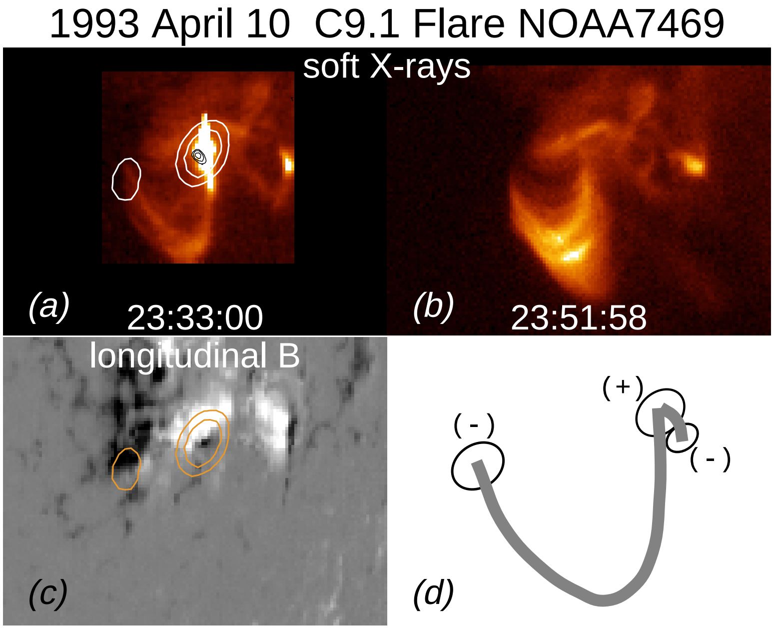

Figure 4—Images of a C9·1 flare at 23:35, 1993 April 10, exhibiting parasitic magnetic topology. This figure is adapted from Figure 3 of Hanaoka (1997). In panel (a) the Yohkoh SXR image of the flare around the peak of the flare is shown, with microwave contours overlaid in white, and HXR contours overlaid in black. In panel (b) the Yohkoh SXR image in the decay phase of the flare is shown. In panel (c) the longitudinal magnetogram from Kitt Peak Observatory at 19:00 on April 10 is shown with the microwave contours overlaid. Panel (d) is a sketch of the geometry suggested by both the displayed images and the microwave polarisation data. For further details see Hanaoka (1997).

In Figure 2 we present three plots of the energy released between pre- and post-flare configurations within the model of M97; the positions of three of the footpoints, 1+, 1− and 2−, are fixed in the geometry shown in Figure 4d. The position of the fourth footpoint, 2+, is allowed to vary within the plane. The three plots correspond to three different ratios, $r = I_1/I_2$, where I_1 is the current in the longer loop (loop 1). Clearly, on energetic grounds, a flare is allowed for all three values of r. Thus, based purely on geometry, the model of M97 is not sufficient to constrain the flare events to a particular current ratio. The model of M97 demonstrates that current transfer within a parasitic configuration leads to a reduction in the stored magnetic energy, and thus is a favourable configuration for flares.

There are further constraints we may investigate by restricting our attention to a single configuration of footpoints. In Figure 5 the location of all four footpoints is specified as shown and the energy released is plotted against the ratio of the currents in the two loops. A strong peak in the amount of energy released occurs when the smaller loop carries around twice the current of the long loop. The existence of a correlation between the ratio of currents and the energy release in a flare in parasitic topologies is a strong prediction of the theory of M97, and is subject to experimental verification. For strong flares, current maps may be generated from magnetogram data and combined with X-ray and microwave data to determine the locations of the footpoints and the currents passing through them. These may then be used as inputs for the theory and the predicted energy release may be compared against the total energy released in the flare. Such a program is under way.

We note that Figure 5 corresponds only to a particular footpoint configuration. Other configurations that we have examined also show a strong dependence on the ratio of currents in the loops.

Another effect that may be important is incomplete current transfer between the loops. Figure 6 shows a plot of the energy released as a function of both the current ratio r and the fraction of the total allowed current that is transferred. As noted in Section 2, incomplete current transfer is likely for a variety of reasons. Figure 6 demonstrates that the total energy release remains a strong function of the ratio of currents for all but the smallest current transfers.

We conclude that flares which exhibit parasitic magnetic topology, often associated with emerging flux loops, form a class of events that may be used to observationally test the theory of M97.

https://doi.org/10.1071/AS98318

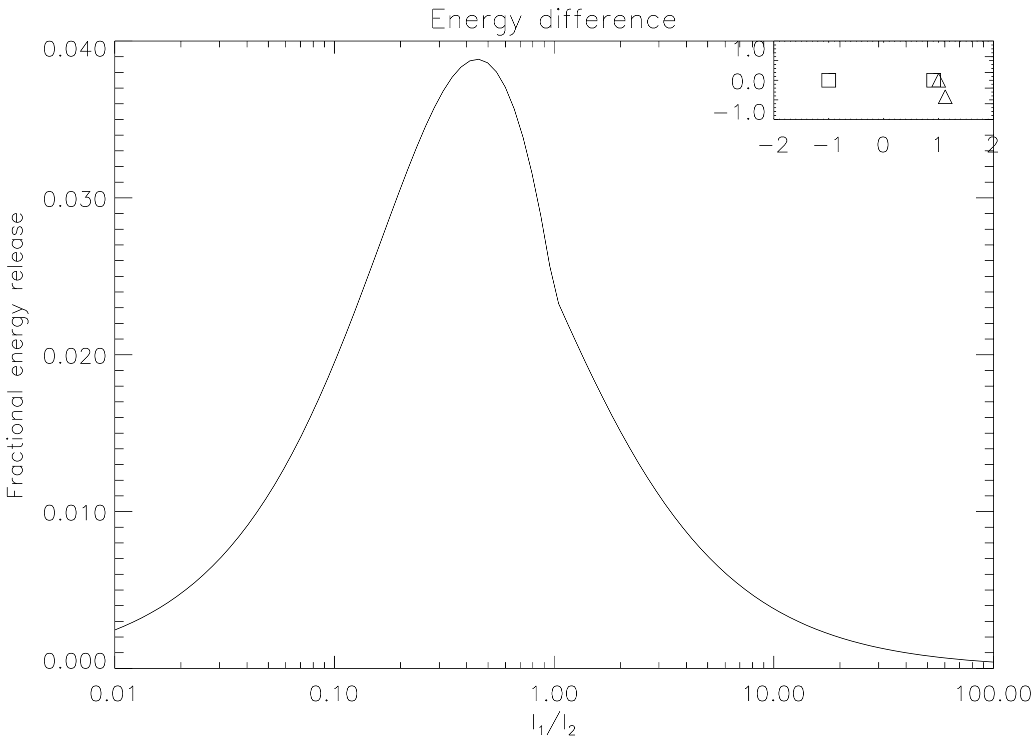

Figure 5—Plot of the fractional energy released, for the configuration shown at top right, as a function of the ratio of currents in the two initial loops. Though energy is released for any ratio, the amount of energy released is a strong function of the ratio, and thus stronger flares should be expected where the current in the smaller loop is approximately twice the current in the larger loop.

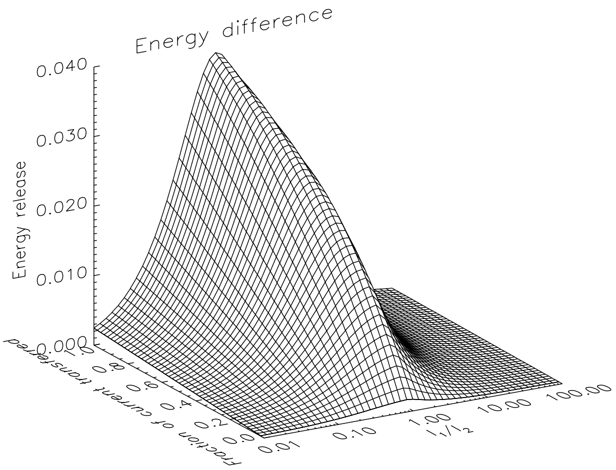

Figure 6—Plot of the fractional energy released, for the configuration shown in Figure 5, as a function of the ratio of currents in the two initial loops and of the proportion of the maximal current transferred. The energy released is a strong function of the ratio of currents for all but the smallest current transfers. Thus larger energy releases should be expected for a stronger smaller loop, regardless of the size of the current transfer.

3.2 Formation of Long Flux Tubes between Active Regions

A further application of this theory, suggested by M97, is to the formation of long flux tubes between active regions. The proposed mechanism is that an existing flux loop interacts with a flux loop in a network field element or an ephemeral active region, reconnecting to produce a longer loop. A sequence of these events would lead to the formation of a long loop connecting active regions. Figure 7 shows the energy release for two configurations with three fixed footpoints: the first loop from $(-1, 0)$ to $(1, 0)$; the second loop with the positive footpoint fixed at $(0{\cdot}7, 0)$ in (a) and the negative footpoint fixed at $(0{\cdot}7, 0)$ in (b). In both the plots, the currents in the initial loops are assumed equal. In Figure 7a we see that energy release is possible for essentially any configuration that makes the loop longer, but not for the configurations that make the loops shorter. In Figure 7b we see that if the footpoint of the ephemeral emerging flux loop which is between the loops is negative in polarity, energy release is negative for the majority of initial conditions. Thus, these long flux loops should appear as the result of interactions between loops where the footpoint of the emerging flux is of opposite polarity to the nearest footpoint of the existing loop. This claim of the theory of M97 may be tested using a combination of X-ray and magnetogram data.

3.3 Largest Energy Release

There are various footpoint configurations and current ratios which lead to energy release. Animations of the fractional energy release for a large class of

https://doi.org/10.1071/AS98318

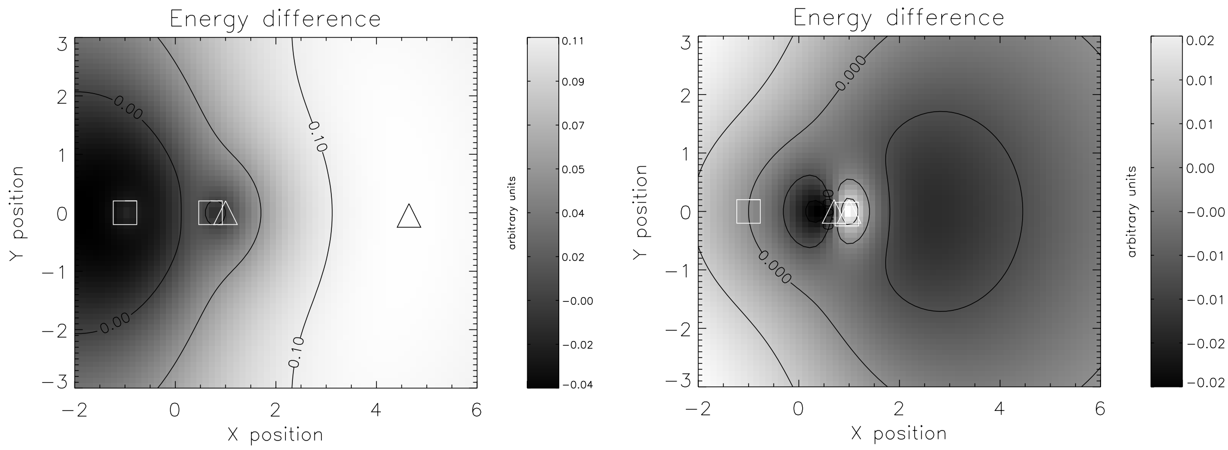

Figure 7—A plot of the fractional energy release for two configurations where the footpoint of one flux loop is between the two footpoints of another flux loop. These plots demonstrate that if an ephemeral flux loop appears in such a configuration the majority of favourable configurations for flares and current transfer involve increasing the size of the loop. Thus, this provides a mechanism for the creation of the long flux loops connecting active regions which are observed.

initial conditions have been calculated. They may be obtained from S. J. H. on request. The interested reader is directed to these animations for a more complete description of the predictions for energy release of equation (1).

4 Conclusion

In our exploration of the model of M97 we show that a number of observational tests may be applied to the model to determine the validity of the underlying theory. These include:

1. Any flare event in which the loop's structure and footpoint location can be determined may be modelled through the theory of M97. A test based on this geometry may be applied to determine whether or not current transfer leads to energy release, and under what conditions on the currents in the loops. Some geometries are unfavourable for energy release regardless of the current ratio in the loop, and flares from such geometries are ruled out by the model.
2. If magnetogram data of sufficient quality have been taken for the active region in which the flare occurs, the currents flowing through the flux loops may be determined. This fully specifies the model of M97, and a comparison between the predicted energy release and the observed energy release may be made.
3. For flares which occur in parasitic geometries, the model of M97 predicts a strong correlation between the energy released in a flare and the ratio of the currents in the interacting loops. This prediction may be tested by examining a number of such flares with a wide range of energies, and looking for correlations between the energy of the flares and the currents in the loops. Application of this approach is hampered by the difficulty in measuring the currents passing through the photosphere directly, and an indirect method of estimating the relative sizes of the currents in the loops may be required.
4. The model of M97 suggests a mechanism for the formation of long flux loops connecting active regions. This mechanism may be tested directly against Yohkoh SXR observations of the formation of these loops.

A number of these observational analyses are under way.

Acknowledgments

The authors thank Y. Hanaoka for supplying Figure 4.

References

Hanaoka, Y. 1997, Solar Phys., 173, 319
Heyvaerts, J., Priest, E. R., & Rust, D. M. 1977, ApJ, 216, 123
Machado, M. E., Moore, R. L., Hernandez, A. M., Rovira, M. G., Hagyard, M. J., & Smith, J. B. Jr 1988, ApJ, 326, 425
Melrose, D. B. 1997, ApJ, 486, 521 (M97)
Nishio, M., Yaji, K., Kosugi, T., Nakajima, H., & Sakurai, T. 1997, ApJ, 489, 976